Proc. of JSCE No. 451/V-17, pp. 301~311, August 1992

MODIFIED CYCLIC MICROMECHANICAL MODEL FOR CONCRETE

Ahmed M.FARAHAT*, Zhishen WU**
and Tada-aki TANABE***

A detailed cyclic micromechanical model based on the micromechanics of granular material is proposed for concrete. In the current study, concrete is idealized to have two kinds of contacts ; aggregate-aggregate and aggregate- mortar contacts. The behavior of these contacts is examined and distinguished for both cyclic and virgin loadings. Finally, an explicit formula which expresses the tangent stiffness matrix of the material as a summation of the contributions of all contacts inside any representative volume is derived. Moreover, the nonhomogeniety of the microstructure and the nonuniformity of strain distribution are considered. This is in contrast to Bazant's microplane model in which concrete has been treated as a homogenous brittle aggregate material having a single kind of contact with uniform strain distribution.

Keywords : *concrete, cyclic, nonhomogeniety, micromechanics, aggregate and mortar*

1. INTRODUCTION

During the last two decades we have witnessed a tremendous progress in the development of constitutive models to investigate the characteristics of concrete. At present the existing models are basically two kinds : (1) macroscopic models, in which the constitutive relation is formulated in terms of the macroscopic continuum stress and strain tensors and their invariants ; and (2) microscopic models, in which the micromechanics of deformation is described by some suitably simplified model and the constitutive material properties are characterized by a relation between the stress and strain components (or forces and displacements) on the microlevel. The former one is the classical approach, which has led to important advances in the modeling of concrete. However, the more realistic macroscopic constitutive models for concrete are rather complicated and very difficult to identify from test data, since they contain many material parameters ; while the agreement with test data is still less than satisfactory. In addition, in the calculation of the most of macroscopic models, concrete was treated as a homogenous material and the strain distribution was considered to be uniform. Also, the macroscopic models for cyclic loading are based on the fitting of the test data, so, once a new set of experimental data is observed, a new model for cyclic loading has to be proposed. However, concrete is a complex and extremely heterogeneous material, whose fracture and failure strengths depend on the strength, size, quantity, and distribution of aggregate as well as the quality of the mortar used.

The second kind of material models, which is based on the micromechanics of the inelastic behavior in the material microstructure seems to be more promising. The main reason is, the micromechanical models enable us to look into far insight of the true damage or the failing mechanisms of concrete under the effect of static and cyclic loading. Moreover, through the micromechanical models the nonhomogeniety of the material and the nonuniformity of strain distribution can be considered. In addition, the cyclic micromechanical models are more realistic and it can be generalized.

Micromechanical models were analyzed for different kinds of materials such as granular materials, metals, and concrete. Routhenburg et al.[1], Chang et al.[2] and Christoffersen et al.[3] investigated the micromechanical behavior of granular materials. In their studies, only one kind of particle and one kind of contact were considered. In the microplane model proposed by Bazant et al.[4] Concrete has been treated as a brittle aggregate material. Moreover, the tangent stiffness matrix of the material has been expressed as an integral over the surface of unit hemisphere. Therefore, only the aggregate-aggregate contact has been taken into account. Also in their model, the microstructure was assumed to be homogenous and the strain distribution was considered to be uniform. In the author's previous work[5] although two kinds of contact surfaces were formulated, the contacts were supposed to have the same properties. Also, the microstructure was considered to

* Student member of JSCE Dipt. of Civil Eng., Nagoya University (Nagoyo 464, Japan)
** Member of JSCE, Dr. Eng. Assist. Prof., Nagoya University
*** Member of JSCE, Dr. Eng., Professor, Nagoya University

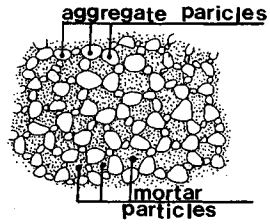

Fig.1 Idealized Distribution of Particles in Concrete

n^{AB} = contact normal
l^{AB} = contact vector
f^{AB} = contact force

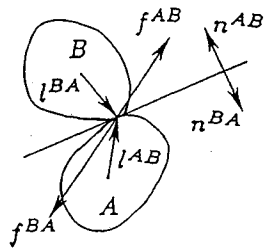

Fig.2 Contact Force, Contact Normal and Contact Vector

be homogenous and the strain distribution was treated to be uniform.

In the present study, as a continuation of the developments of the microscopic models, the micromechanical model of concrete[5] is modified. To represent the different kinds of contacts, concrete is idealized to have two kinds of particles which are aggregate and mortar particles (refer to **Fig.1**). This idealization helps us to investigate the micromechanical behavior not only on the contacts between aggregates as studied before by Bazant et al.[4] but also on the contacts between aggregate and mortar particles. The microstructure is considered to be nonhomogenous and the strain distribution is assumed to be nonuniform. In addition, in the calculation of the stiffness matrix of the microstructure, the contribution of all contacts inside any repesentative volume is superimposed. The constitutive properties by a relation between the normal stresses and the normal strains acting on a plane of any orientation within the microstructure are defined and distinguished. Moreover, these relations can represent both cyclic and static behavior of the different contacts. In addition, to explain the behavior more precisely, shear strain on the contact is considered. The current formulation is capable of predicting the available macroscopic cyclic and static experimental data of concrete.

2. THEORETICAL CONSIDERATIONS

(1) AVERAGE STRESS TENSOR FROM AVERAGES OF CONTACT FORCES

As explained before[5] if in a region v there is stress state σ_{ij}, which is in equilibrium but otherwise may be arbitrarily distributed, the average stress $\bar{\sigma}_{ij}$ is defined[1)~3)] as :

$$\bar{\sigma}_{ij}=\frac{1}{v}\int_v \sigma_{ij}dv \quad \cdots\cdots(1)$$

In this study, concrete is idealized to have plural types of particles, aggregate and mortar, and every mortar particle is assumed to be surrounded by a number of aggregate particles as shown in **Fig.1.** Using the divergence theorem and the equilibrium condition (i.e. $\sigma_{ij,j}=0$), the volume average integral in Eq.(1) can be reduced to the next form[5] :

$$\bar{\sigma}_{ij}=\frac{1}{v}\sum_{m=1}^{n} f_i^m x_j^m \quad \cdots\cdots(2)$$

where n is the number of contacts per particle, both x_j and f_i are the contact vector and the contact force at the m^{th} contact. The contact vector can be measured from the centroid of the particle to the contact point[1)~3)]. The average stress increments within the aggregate and mortar particles can now be written as :

$$\Delta\bar{\sigma}_{ij}^a=\frac{1}{v^a}\sum_{\alpha_1}\Delta f_i^{\alpha_1} l_j^{\alpha_1} \quad \Delta\bar{\sigma}_{ij}^m=\frac{1}{v^m}\sum_{\alpha_2}\Delta f_i^{\alpha_2} l_j^{\alpha_2} \quad (3)$$

where α_1 and α_2 are the notations to identify each contact point along the boundary, and l_j is the contact vector as shown in **Fig.2.**, v^a and v^m are the volume of an aggregate and mortar particles, respectively. Furthermore, the average volume will be used to define the incremental mean stress on any volume by summing the incremental stresses on all particles within the volume as follows

$$\Delta\bar{\sigma}_{ij}=\frac{1}{V}\left[\sum_a \Delta\bar{\sigma}_{ij}^a v^a+\sum_m \Delta\bar{\sigma}_{ij}^m v^m\right] \quad \cdots\cdots(4)$$

Eq.(4) can be simplified to next form :

$$\Delta\bar{\sigma}_{ij}=\frac{1}{V}\left[\sum_{C_1}\Delta f_i^{c1} l_j^{c1}+\sum_{C_2}\Delta f_i^{c2} f_j^{c1}+\sum_{C_2}\Delta f_i^{c2} l_j^{c2}\right] \quad \cdots\cdots(5)$$

where C_1 and C_2 are the total number of contacts between aggregates alone and between aggregate and mortar particles, respectively. V is the total volume.

The total number of contacts do not take into account the orientation of contact normals. Because the case of two dimensional system is considered in the current study, a function $E(\theta)$ is defined to consider the relative frequency of contacts with different orientation. The number of contacts with normals between θ and $\theta+\Delta\theta$ will be $CE(\theta)\Delta(\theta)$. This function satisfies that $\int_0^{2\pi} E(\theta)d\theta=1$. If the contacts are grouped within a finite number of orientational intervals, then, the grouped averages $\Delta\bar{f}(\theta)$ in Eq.(5) can be calcu-

lated. For a large number of contacts and very small orientational intervals $\Delta\theta$, Eq.(5) can be written as :

$$\Delta\bar{\sigma}_{ij}=\frac{1}{V}\Big[\sum_{\theta_g}\Delta\bar{f}_i^{c1}\bar{l}_j^{c1}(\theta)\,(C_1E(\theta)\Delta\theta) + \sum_{\theta_g}\Delta\bar{f}_i^{c2}\bar{l}_j^{c1}(\theta)\,(C_2E(\theta)\Delta\theta) + \sum_{\theta_g}\Delta\bar{f}_i^{c2}\bar{l}_j^{c2}(\theta)\,(C_2E(\theta)\Delta\theta)\Big] \cdots\cdots (6)$$

Assuming that the number or contacts is very large, while the orientational interval $\Delta\theta$ is very small, Eq.(6) can be expressed in the next integral form :

$$\Delta\bar{\sigma}_{ij}=\frac{C_1}{V}\int_0^{2\pi}\Delta\bar{f}_i^{c1}\bar{l}_j^{c1}(\theta)E(\theta)d\theta + \frac{C_2}{V}\int_0^{2\pi}\Delta\bar{f}_i^{c2}\bar{l}_j^{c1}(\theta)E(\theta)d\theta + \frac{C_2}{V}\int_0^{2\pi}\Delta\bar{f}_i^{c2}\bar{l}_j^{c2}(\theta)E(\theta)d\theta \cdots\cdots (7)$$

Since $\bar{l}_j(\theta)=\bar{l}n_j(\theta)$, and considering that $\bar{l}_1$ and $\bar{l}_2$ are the averages of the radii of aggregate and mortar particles respectively, Eq.(7) can be rewritten in the next form :

$$\Delta\bar{\sigma}_{ij}=\frac{C_1\bar{l}_1}{V}\int_0^{2\pi}\Delta\bar{f}_i^{c1}(\theta)n_j(\theta)E(\theta)d\theta + \frac{C_2\bar{l}_1}{V}\int_0^{2\pi}\Delta\bar{f}_i^{c2}(\theta)n_j(\theta)E(\theta)d\theta + \frac{C_2\bar{l}_2}{V}\int_0^{2\pi}\Delta\bar{f}_i^{c2}(\theta)n_j(\theta)E(\theta)d\theta \cdots\cdots (8)$$

To consider the nonhomogeniety of the microstructure, several cross sections of concrete have been observed and the orientational distribution function $E(\theta)$ of the contact normals was found to be as follows :

$$E(\theta)=\frac{1}{2\pi}[1+A\cos^2\theta-A\sin^2\theta] \cdots\cdots (9)$$

where A is the nonhomogeniety parameter (refer to **Fig.3**). Based on ref[6] it was found that the value of A varies from -0.15 to $+0.15$. To measure the function $E(\theta)$, the contact normals within the microstructure are divided into several groups with an orientational intervals $\Delta\theta=10°$. For each interval, the number of contact normals is counted and its fraction with respect to the total number of contact normals is calculated and plotted as shown in **Fig.3**. The total number of contact normals is obtained by summing the contact normals in all intervals.

(2) RELATION BETWEEN AVERAGE CONTACT FORCES AND STRAIN TENSOR

Neglecting the possible rotation between particles, the average contact force increment is linked with the contact desplacement increment using the linear contact law as follows :

$$\Delta f_n^c=K_{nn}\Delta\left(\frac{\delta_n^c}{l}\right),\quad \Delta f_s^c=K_{ss}\Delta\left(\frac{\delta_t^c}{l}\right) \cdots\cdots (10)$$

where (δ_n^c/l) and (δ_t^c/l) are the relative normal and tangential displacement increments at the contact as shown in **Fig.4**, K_{nn} and K_{ss} refer to the normal and shear stiffnesses of contact, Δf_n and Δf_s are the components of contact force increments and l is the distance between particle centers in contact. Eq.(8) for the average incremental stress tensor contains only the averages of forces increments of same orientations. If $\bar{\delta}_n^c(\theta)$ and $\bar{\delta}_t^c(\theta)$ are the average normal and shear displacement increments of groups of contacts having the same orientations, Eq.(10) can take the next form :

$$\Delta\bar{f}_n^c(\theta)=K_{nn}\Delta\bar{\delta}_n^c(\theta),\quad \Delta\bar{f}_s^c(\theta)=K_{ss}\Delta\bar{\delta}_t^c(\theta) \cdots\cdots (11)$$

where $\bar{\delta}_n^c(\theta)=(\delta\bar{l}_n(\theta)/l)$ and $\bar{\delta}_t^c(\theta)=(\delta\bar{l}_t(\theta)/l)$

Here, the normal and shear microstrian $(\varepsilon_n, \varepsilon_t)$, which govern progressive cracking and failure of microstructure, are assumed to be equal to the resolved components of macroscopic strains and are defined as follow :

$$\varepsilon_n^{aa}=\frac{\delta l_n^{aa}}{l}=K\bar{\varepsilon}_{ij}n_in_j,\quad \varepsilon_t^{aa}=\frac{\delta l_t^{aa}}{l}=K\bar{\varepsilon}_{ij}t_in_j \cdots\cdots (12)$$

$$\varepsilon_n^{am}=\frac{\delta l_n^{am}}{l}=\bar{\varepsilon}_{ij}n_in_j,\quad \varepsilon_t^{am}=\frac{\delta l_t^{am}}{l}=\bar{\varepsilon}_{ij}t_in_j \cdots\cdots (13)$$

where (ε_n^{aa} and ε_t^{aa}) and (ε_n^{am} and ε_t^{am}) are the normal and shear strains at the contact between aggregate-aggregate and aggregate-mortar particles, respectively. $\bar{\varepsilon}_{ij}$ is the total average strain, n and t are the direction cosines of the unit normal and unit tangent of the contact, i.e. $n=(\cos\theta, \sin\theta)$ and $t=(-\sin\theta, \cos\theta)$ and K is the nonuniformity of strain distribution parameter (i.e. for the same orientation, the strain on the aggregate-aggregate contact is different from that on the aggregate-mortar contact). It was found[6] that the value of K varies from 0.70 to 1.40. It can be expected that Eqs.(12) and (13) will hold true when expressed as averages taken over the contacts of similar orientations as follows :

$$\left.\begin{aligned}\Delta\bar{\delta}_n^{aa}(\theta)&=\Delta\left(\frac{\delta\bar{l}_n^{aa}(\theta)}{l}\right)=K\Delta\bar{\varepsilon}_{ij}n_in_j,\\ \Delta\bar{\delta}_t^{aa}(\theta)&=\Delta\left(\frac{\delta\bar{l}_t^{aa}(\theta)}{l}\right)=K\Delta\bar{\varepsilon}_{ij}t_in_j\\ \Delta\bar{\delta}_n^{am}(\theta)&=\Delta\left(\frac{\delta\bar{l}_n^{am}(\theta)}{l}\right)=\Delta\bar{\varepsilon}_{ij}n_in_j,\end{aligned}\right\} \cdots\cdots (14)$$

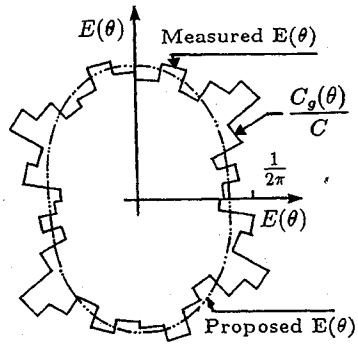

Fig.3 Distribution of Contact Normals

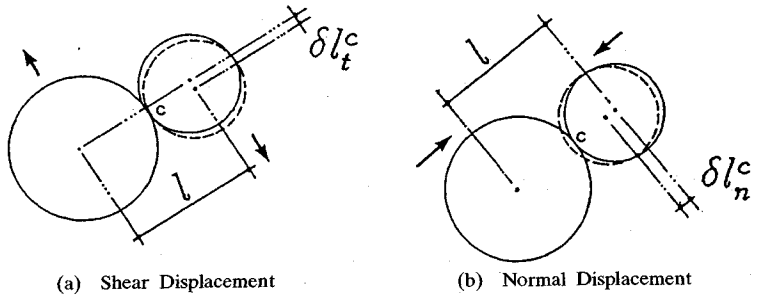

Fig.4 Contact Displacement Components

$$\Delta\bar{\delta}_t^{qm}(\theta)=\Delta\left(\frac{\delta\bar{l}_t^{qm}(\theta)}{l}\right)=\Delta\bar{\varepsilon}_{ij}t_i n_j \quad \cdots\cdots (15)$$

(3) STRESS-STRAIN RELATIONSHIP

In the previous work[5] in which all contacts have been assumed to have the same properties and both the nonhomogeniety of the microstructure and the nonuniformity of strain distribution have not been considered, a simple formula for the stress-strain relationship was derived. However, in the current study, if the average normal and tangential contact force increments in Eq.(11) are combined with Eqs.(14) and (15) and the resulting value is introduced into Eq.(8), the following incremental stress strain relationship can be obtained as follows :

$$\Delta\bar{\sigma}_{ij}=D_{ijkl}\Delta\bar{\varepsilon}_{kl} \quad \cdots\cdots (16)$$

where $D_{ijkl}=\eta_1\int_0^{2\pi}(k_n a_{ijkl}+k_s b_{ijkl})^{c_1}\bar{E}(\theta)Kd\theta$

$$+\eta_2\int_0^{2\pi}(k_n a_{ijkl}+k_s b_{ijkl})^{c_2}\bar{E}(\theta)d\theta,$$

$$a_{ijkl}=n_i n_j n_k n_l, \quad b_{ijkl}=t_i n_j t_k n_l,$$

$$\eta_1=C_1\bar{l}_1\bar{a}_1/2\pi V,$$

$$\eta_2=C_2\bar{l}_1\bar{a}_2/2\pi V+C_2\bar{l}_2\bar{a}_2/2\pi V,$$

$$k_n=K_{nn}/\bar{a}, \quad k_s=K_{ss}/\bar{a},$$

$$\bar{E}(\theta)=2\pi E(\theta)=1+A\cos^2\theta-A\sin^2\theta$$

Both C_1 and $\bar{a}_1$ refer to the contact and the average contact area between aggregate-aggregate, while both C_2 and $\bar{a}_2$ refer to the contact and the average contact area between aggregate-mortar particles, respectively. $\bar{a}$ is the average contact area at either aggregate-aggregate contact (i.e. $\bar{a}=\bar{a}_1$) or aggregate-mortar contact (i.e. $\bar{a}=\bar{a}_2$). k_n and k_s are the normal and shear stiffnesses which can be obtained through the stress-strain relationship on the contact.

(4) NORMAL AND SHEAR STIFFNESSES OF THE CONTACTS (k_n and k_s)

Normal and shear stiffnesses of the contacts are taken as follows :

$$k_n=\frac{d\sigma_n}{d\varepsilon_n}, \quad k_s=\frac{d\tau_{nt}}{d\varepsilon_{nt}} \quad \cdots\cdots (17)$$

where σ_n and ε_n are the normal stress and the normal strain on the contact, τ_{nt} and ε_{nt} are the shear stress and the shear strain on the contact. Here, we made an assumption that k_s is to be linear with k_n (i.e. $k_s=\lambda k_n$). This assumption will be valid in tension and compression.

(5) NORMAL STRESS AND NORMAL STRAIN RELATIONSHIP ON THE TWO KINDS OF CONTACTS

a) Virgin loading behavior of both contacts

Aggregate-Mortar Contact : The stress strain relation for the contact, relating σ_n to ε_n must describe the cracking and the damage all the way to complete fracture or failure, at which σ_n reduced to zero. It is clear that σ_n as a function of ε_n must first rise, then reach a maximum, and then gradually decline to zero. The final zero vlaue is chosen to be attained asymptotically, since no precise information exists on the final strain at which $\sigma_n=0$, and since a smooth curve is convenient computationally. The following expressions are used (refer to **Fig.5 (a)**)

for $\varepsilon_n\geq 0$ $\quad \sigma_n=E_2\varepsilon_n\exp\left[-k_t\left(\frac{E_2}{E_1}\right)^p(\varepsilon_n)^p\right]$

$\cdots\cdots (18)$

for $\varepsilon_n\leq 0$ $\quad \sigma_n=E_2\varepsilon_n\exp[-k_c|\varepsilon_n|^{p_1}]$

$\cdots\cdots (19)$

where k_t, k_c, p, and p_1 are positive constants, E_1 and E_2 are the initial stiffnesses of aggregate-aggregate contact and aggregate-mortar contact, respectively.

Aggregate-Aggregate Contact : To describe the behavior on the aggregate-aggregate contact, the normal stress-normal strain relationship proposed by Bazant[4] is used as follows (refer to **Fig.5 (b)**).

for $\varepsilon_n\geq 0$ $\quad \sigma_n=E_1\varepsilon_n\exp[-k_t(\varepsilon_n)^p]$ $\cdots\cdots (20)$

for $\varepsilon_n\leq 0$ $\quad \sigma_n=-C_1+C_2\tan^{-1}[C_3(\varepsilon_n-C_4)]$

$\cdots\cdots (21)$

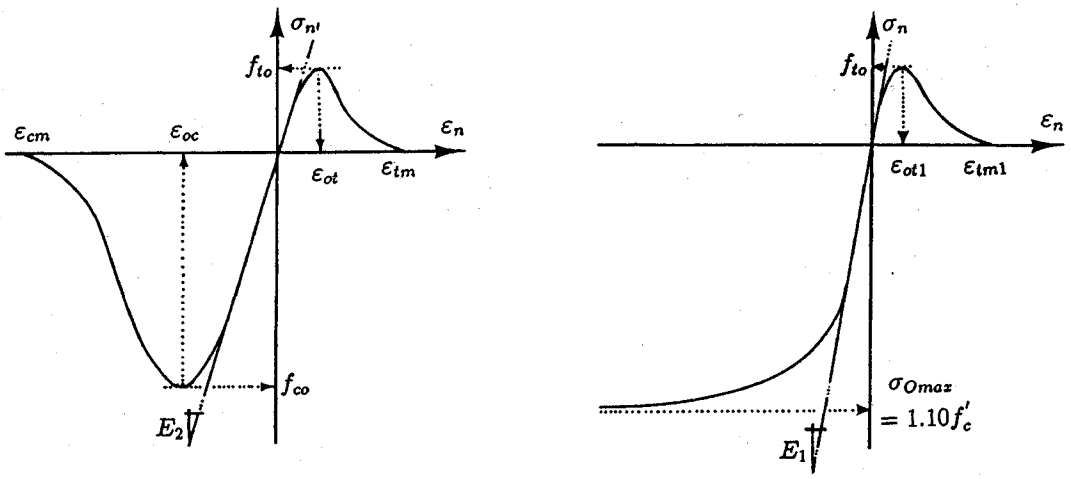

(a) Aggregate-Mortar Contact (b) Aggregate-Aggregate Contact

Fig.5 Virgin Loading Behavior of Both Contacts

where : $\sigma_0=\dfrac{1.86+15.0\times10^5(\varepsilon^*)^{2.5}}{1.00+15.0\times10^5(\varepsilon^*)^{2.5}}(0.58f_c')$

$C_2=0.334\sigma_0[1.0+1.38\exp(-400\varepsilon^*)]$

$C_1=\sigma_0-C_2\left(\dfrac{\pi}{2}\right)$,

$C_3=\dfrac{0.07}{C_2}[1.0+13.29$

$\exp\{-14(\varepsilon^*)^{0.30}\}]E_1$,

$C_4=\varepsilon^*-\dfrac{1}{C_3}\tan\dfrac{\sigma^*+C_1}{C_2}$

In Eq.(21) the values of ε^* and σ^* are equal to zero when it will be used for monotonic loading.

b) Cyclic Loading

1) Unloading Path from Tension

Based on the experimental data[8)~12)], the following unloading and reloading paths are assumed :

Aggregate-Mortar Contact : In the unloading from tension to compression, depending on the coordinates of the reloading point in the previous cycle, either path (A) or path (B) will be followed as shown in **Fig.7**(a). Path (A), in which the compressive stress at the reloading point in the previous cycle is higher than the peak stress, the following path is assumed[8),9),10)].

$$\sigma_n=\sigma^*+\left[\frac{f_{t0}}{3\left(\dfrac{\varepsilon^*}{\varepsilon_{tm}}\right)+0.40}\right]\left[0.02\left\{\ln\left(\frac{\varepsilon_n+\varepsilon_{rc}}{\varepsilon^*+\varepsilon_{rc}}\right)\right\}^5-0.80\left(\frac{\varepsilon_{tm}}{\varepsilon^*}\right)\sqrt{\frac{\varepsilon^*-\varepsilon_n}{\varepsilon^*+\varepsilon_{rc}}}\right] \quad \cdots\cdots (22)$$

where : $\varepsilon_{rc}=\left(\dfrac{f_{c0}}{E_2}\right)-\varepsilon_c$, $\varepsilon_c=\left(\varepsilon_{0t}-\left(\dfrac{f_{c0}}{E_2}\right)\right)$

$(1.0-\exp\{-C\varepsilon_{cr}\})$

$\varepsilon_{cr}=\varepsilon^*-\varepsilon_{irr}-\left(\dfrac{\sigma^*}{E_2}\right)$, $\varepsilon_{irr}=\varepsilon_{0t}-\left(\dfrac{f_{t0}}{E_2}\right)$,

$\varepsilon_{tm}\approx5\varepsilon_{0t}$ $\varepsilon_{tm1}\approx5\varepsilon_{0t1}$

where ε^* and σ^* are the coordinates of the unloading point and C is a parameter to control the position of the peak compressive strength point as shown in **Fig.6**. Beyond the peak stress, the following path is assumed :

$$\sigma_n=S_0-S_0\left(\frac{\varepsilon_{cc}-\varepsilon_n}{\varepsilon_{cc}-\varepsilon_{cm}}\right)^2 \quad \cdots\cdots (23)$$

where $\varepsilon_{cm}\approx4\varepsilon_{0c}$ and S_0 represents the reduced compressive strength due to tensile cracking. This reduction is considered to be similar to ref.[4)] as follows :

$$S_0=\frac{1.86+15.0\times10^5(\varepsilon^*)^{2.5}}{1.00+15.0\times10^5(\varepsilon^*)^{2.5}}(0.538f_{c0})$$

For path (B) as shown in **Fig.7**(a), in which the compressive stress at the reloading point in the previous cycle exceeded the peak compressive strength (i.e. in the softening zone). Path (B) is assumed to follow the next form :

$$\sigma_n=\sigma^*+(\sigma_r-\sigma^*)\left\{\frac{\varepsilon_n-\varepsilon^*}{\varepsilon_r-\varepsilon^*}\right\}^{0.70} \quad \cdots\cdots (24)$$

where $\varepsilon_r=\varepsilon^*+0.02\varepsilon^{**}\left\{\ln\left(1.0+3.0\left(\dfrac{\varepsilon^{**}-\varepsilon^*}{\varepsilon_{0c}}\right)\right)\right\}$

and ε^{**} is the coordinate of the previous cycle.

Aggregate-Aggregate Contact : As proposed by Bazant[4)], Eq.(21) will be used if the unloading in tension occurred on the aggregate-aggregate contact as shown in **Fig.7**(b). It should be noted here that in Eq.(21) both ε^* and σ^* are the coordinates of the unloading point.

2) Reloading Path to Tension

For both aggregate-aggregate contact and aggre-

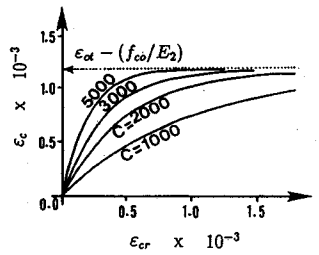

Fig.6 Effect of C Parameter

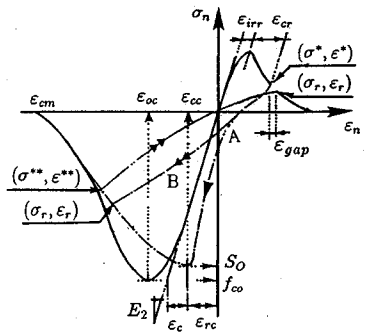

(a) Aggregate-Mortar Contact

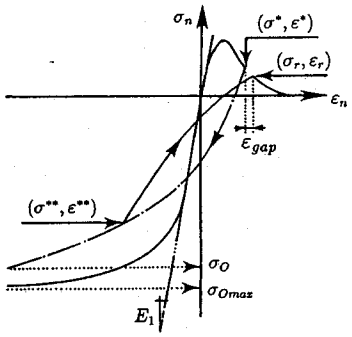

(b) Aggregate-Aggregate Contact

Fig.7 Unloading Path from Tension and Reloading to Tension

gate-mortar contact as shown in **Fig.7**, the gap in the envelope curve is described with an expression similar to the expression proposed by ref.8).

$$\varepsilon_{gap}=0.02\left\{\ln\left(1.0+3.0\left(\frac{\varepsilon^*-\varepsilon^{**}}{\varepsilon_{0t}}\right)\right)\right\} \cdots\cdots (25)$$

where ε_{0t} (or ε_{0t1} in the case of aggregate-aggregate contact) is the strain at the peak tensile strength. The coordinates of the returning point on the envelope curve (σ_r, ε_r) can now be found with

$$\varepsilon_r=\varepsilon^*+\varepsilon_{gap} \cdots\cdots (26)$$

and Eqs.(18) and (20). Starting from the reloading point (σ^{**}, ε^{**}) up to the returning point (σ_r, ε_r) at the envelope curve, the reloading curve is assumed to be as follows :

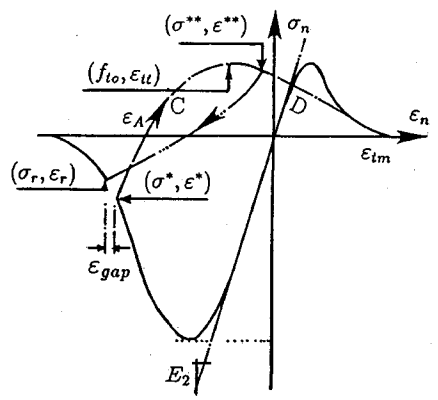

(a) Aggregate-Mortar Contact

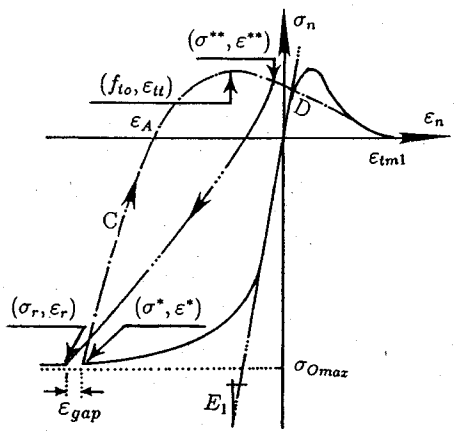

(b) Aggregate-Aggregate Contact

Fig.8 Unloading Path from Compression and Reloading to Compression

$$\sigma_n=\sigma^{**}+(\sigma_r-\sigma^{**})\left\{\frac{\varepsilon_n-\varepsilon^{**}}{\varepsilon_r-\varepsilon^{**}}\right\}^{0.60} \cdots\cdots (27)$$

3) Unloading Path from Compression

Based on the experimental data of ref.12), in which the focal points model was proposed, the coordinates of the intersection point between the unloading curve and the strain axis are obtained and modified to be suitable for microscopic path. Starting from the unloading point (σ^*, ε^*) and passing through the modified point (0, ε_A) up to the maximum tensile strength (f_{to}, ε_{tt}), the unloading curve is assumed to be as follows (refer to path C in **Fig.8**).

$$\sigma_n=\sigma^*-\sigma^*\left\{\frac{\varepsilon_n-\varepsilon^*}{\varepsilon_A-\varepsilon^*}\right\}^{0.60} \cdots\cdots (28)$$

for aggregate-mortar contact

$$\varepsilon_A=\left[1.0+0.20\left(\ln\left\{\frac{\varepsilon_{cm}}{\varepsilon^*}\right\}\right)\right]\left[\frac{\varepsilon^*-(\sigma^*/E_2)}{1+(\sigma^*/f_{c0})}\right]$$

for aggregate-aggregate contact

$$\varepsilon_A=\frac{\varepsilon^*-(\sigma^*/E_1)}{0.70(1.0+(\sigma^*/\sigma_{0max}))},$$

$\sigma_{0max}=1.10f_c'$(Ref. 4))

Bayond the point of maximum tensile strength, a second order curve is assumed to join the point (f_{t0}, ε_{tt}) and the point (0, ε_{tm}) or (0, ε_{tm1}) as shown in **Fig.8** (path D). This curve is defined to be as follows :

$$\sigma_n=f_{t0}-f_{t0}\left\{\frac{\varepsilon_n-\varepsilon_{tt}}{\varepsilon_{tm}-\varepsilon_{tt}}\right\}^2 \cdots\cdots(29)$$

4) Reloading Path to Compression

In a similar manner to reloading to tension, for both aggregate-aggregate contact and aggregate-mortar contact as shown in **Fig.8**, the gap in the envelope curve is described as follows :

$$\varepsilon_{gap}=0.02\left\{\ln\left(1.0+3.0\left(\frac{\varepsilon^*-\varepsilon^{**}}{\varepsilon_{0c}}\right)\right)\right\} \cdots\cdots(30)$$

where ε_{0c} is the strain at the peak compressive strength (ε_{0c} in the aggregate-aggregate contact=(σ_{0max}/E_1)). The coordinates of the returning point on the envelope curve (σ_r, ε_r) can now be found with

$$\varepsilon_r=\varepsilon^*+\varepsilon_{gap} \cdots\cdots(31)$$

and Eq.(19) and (21). Starting from the reloading point (σ^{**}, ε^{**}) up to the returning point (σ_r, ε_r) at the envelope curve, the reloading curve is assumed to be as follows :

$$\sigma_n=\sigma^{**}+(\sigma_r-\sigma^{**})\left\{\frac{\varepsilon_n-\varepsilon^{**}}{\varepsilon_r-\varepsilon^{**}}\right\}^{0.60} \cdots\cdots(32)$$

3. POISSON'S RATIO AND THE RELATION OF INITIAL MACROSTIFFNESS AND MICROSTIFFNESS

To check the value of Poisson's ratio, the case of uniaxial strain is considered (i.e. $\bar{\varepsilon}_x=0$ and $\bar{\varepsilon}_y\neq 0$). Assuming that for small strain $\sigma_n^{aa}=E_1\varepsilon_n^{aa}$ and $\sigma_n^{am}=E_2\varepsilon_n^{am}$, using Eqs.(16) and (17), the following results can be obtained :

$$\bar{\sigma}_x=\left[\eta_1\int_0^{2\pi}E_1(\cos^2\theta\sin^2\theta-\lambda\cos^2\theta\sin^2\theta)(1+A\cos^2\theta-A\sin^2\theta)Kd\theta+\eta_2\int_0^{2\pi}E_2(\cos^2\theta\sin^2\theta-\lambda\cos^2\theta\sin^2\theta)(1+A\cos^2\theta-A\sin^2\theta)d\theta\right]\bar{\varepsilon}_y \cdots\cdots(33)$$

$$\bar{\sigma}_x=\frac{\pi}{4}(1-\lambda)(E_1\eta_1K+E_2\eta_2)\bar{\varepsilon}_y \cdots\cdots(34)$$

$$\bar{\sigma}_y=\left[\eta_1\int_0^{2\pi}E_1(\sin^4\theta+\lambda\cos^2\theta\sin^2\theta)(1+A\cos^2\theta-A\sin^2\theta)Kd\theta+\eta_2\int_0^{2\pi}E_2(\sin^4\theta+\lambda\cos^2\theta\sin^2\theta)(1+A\cos^2\theta-A\sin^2\theta)d\theta\right]\bar{\varepsilon}_y \cdots\cdots(35)$$

$$\bar{\sigma}_y=\frac{\pi}{4}(3+\lambda-2A)(E_1\eta_1K+E_2\eta_2)\bar{\varepsilon}_y \cdots\cdots(36)$$

Therefore, $\bar{\sigma}_x/\bar{\sigma}_y=(1-\lambda)/(3+\lambda-2A)$, and in view of Hook's law $\bar{\sigma}_x/\bar{\sigma}_y=\nu/(1-\nu)$. Then the relation among ν, λ and A, and the relation among the initial macroscopic and microscopic stiffnesses E, E_1 and E_2 are obtained as follows :

$$\nu=\frac{1-\lambda}{4-2A},\quad E=\frac{\pi}{4}(3+\lambda-2A)(\eta_1E_1K+\eta_2E_2) \cdots\cdots(37)$$

Since the elastic Poisson's ratio of concrete is usually taken around 0.20, the relation between the ratio of shear and normal stiffnesses of microplane (i.e. λ) and the parameter corresponding to the nonhomogeniety of microstructure (i.e. A) is $\lambda=0.20+0.40A$.

4. VERIFICATION OF THE VALIDITY OF THE PROPOSED MODEL

(1) GENERAL

To insure the capability of the current model, the available macroscopic monotonic and cyclic experimental data are compared with the results through the proposed model. In the beginning, reasonable values of the parameters which describe the characteristic properties of the contacts are selected. A careful attention has been made to select these parameters to obtain identical initial stiffnesses, peak stresses and reasonable hardening and softening tendencies between the experimental data and the results through the model. The values of these parameters are selected to be as follows ; $p=1.5$ (Eqs.(18), (20)), $p_1=1.75$ (Eq.(19)) and $C=3000$ (Eq.(22)). From ref.7), using the properties of aggregate and motar, the ratio $E_1/E_2=1.80$ and the value of $K=0.80$ (Eq.(14)) can be calculated. Also, the value of $K=0.80$ satisfies the results of ref.6). In Eq.(37), as the ratio η_1/η_2 decreases more softening can be achieved, however, the ratio $\eta_1/\eta_2=0.05$ is used, moreover, the value of $\eta_1+\eta_2=1$ (from ref.5)) is also considered. Based on the results of ref.6), to get identical initial stiffnesses between the test results and the results through the proposed model, the value of $A=0.05$ (Eq.(9)) is selected. In addition, the value of λ in Eq.(37) can be obtained once the value of A is selected. Finally, only k_t and k_c in Eqs.(18), (19) and (20) are considered to be variable parameters.

(2) UNIAXIAL TENSION

In the beginning, by knowing the ratio (η_1/η_2) and (E_1/E_2) and the parameter A as discussed in Section 4.(1), the values of E_1, E_2 and λ which can describe the characteristics of contacts can be obtained by using Eq.(37). The value of $k_c=50\times10^3$ is kept constant while the value of the

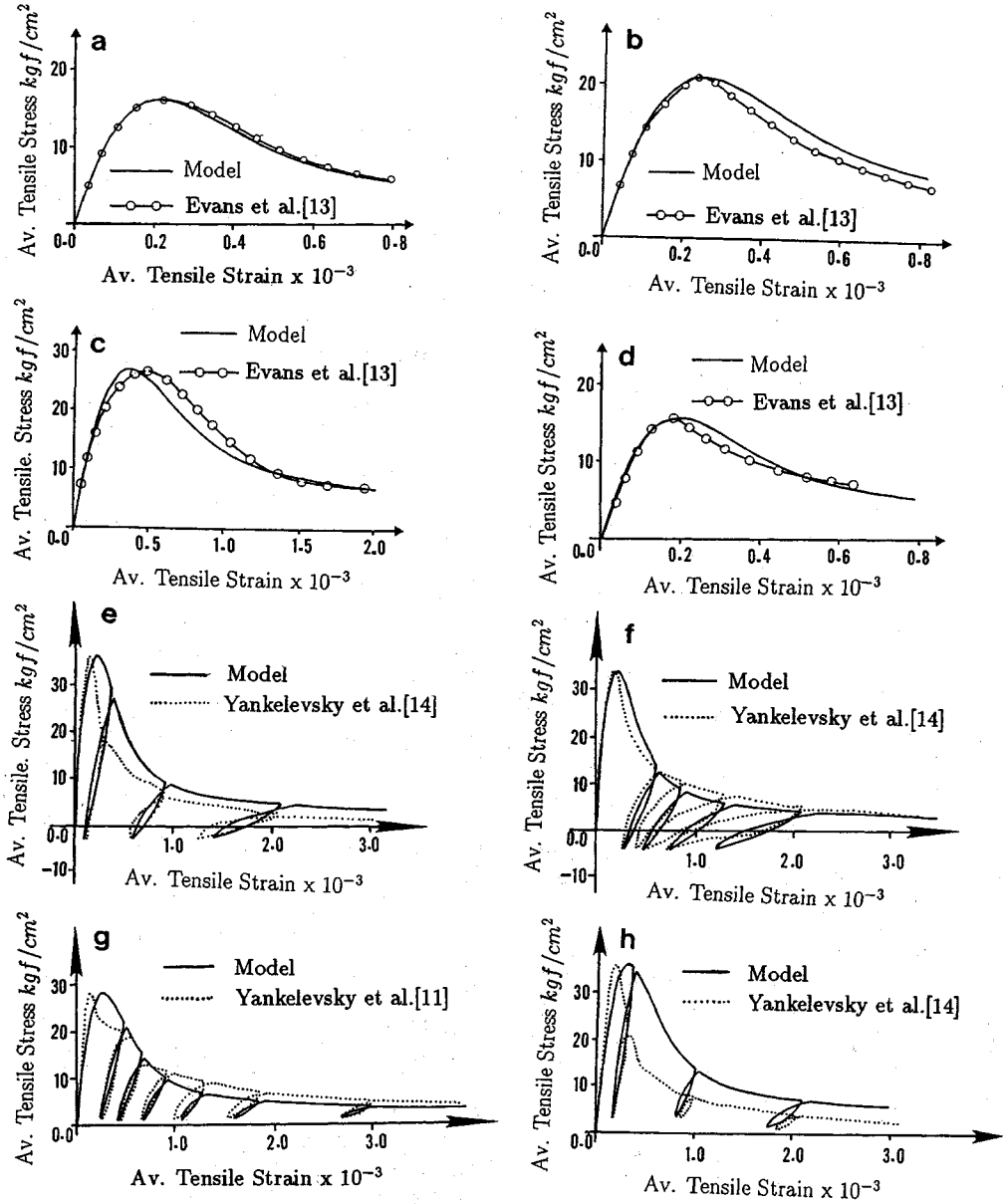

Fig.9 Comparison between Test Data and Model Results (Uniaxial Tension)

parameter k_t is changed to achieve a good fitting of the experimental data, the peak tensile strength of these concretes a, b, c,...h are 16.14, 21.10, 26.70, 15.60, 36.00, 34.00, 27.50 and 36.00 kgf/cm^2, respectively, and the compressive strength is assumed to be 10 times the tensile strength. Also, the values of $10^{-4}E$ (E is the initial macrostiffness) of these concretes are 15.50, 17.50, 15.25, 16.25, 36.00, 35.70, 22.05 and 24.63 kgf/cm^2, respectively. It was found that the values of $10^{-4}k_t$ which can achieve a reasonable fitting of the experimental data for concretes in **Fig.9** (a~h) are 77.00, 62.50, 35.00, 89.00, 73.00, 78.00, 51.50 and 43.50, respectively. For static loading, as can be seen, a good agreement with test data can be obtained although only one parameter (i.e. k_t) is used to fit the test data. The value of the parameter k_t can be obtained through the proposed relation in Section **4.(4)**. For cyclic loading, a reasonable agreement with the test data is also obtained. However, a more comprehensive research must be conducted to observe the cyclic behavior, since the proposed paths are checked with the uniaxial cyclic loading and cyclic tension with low compression.

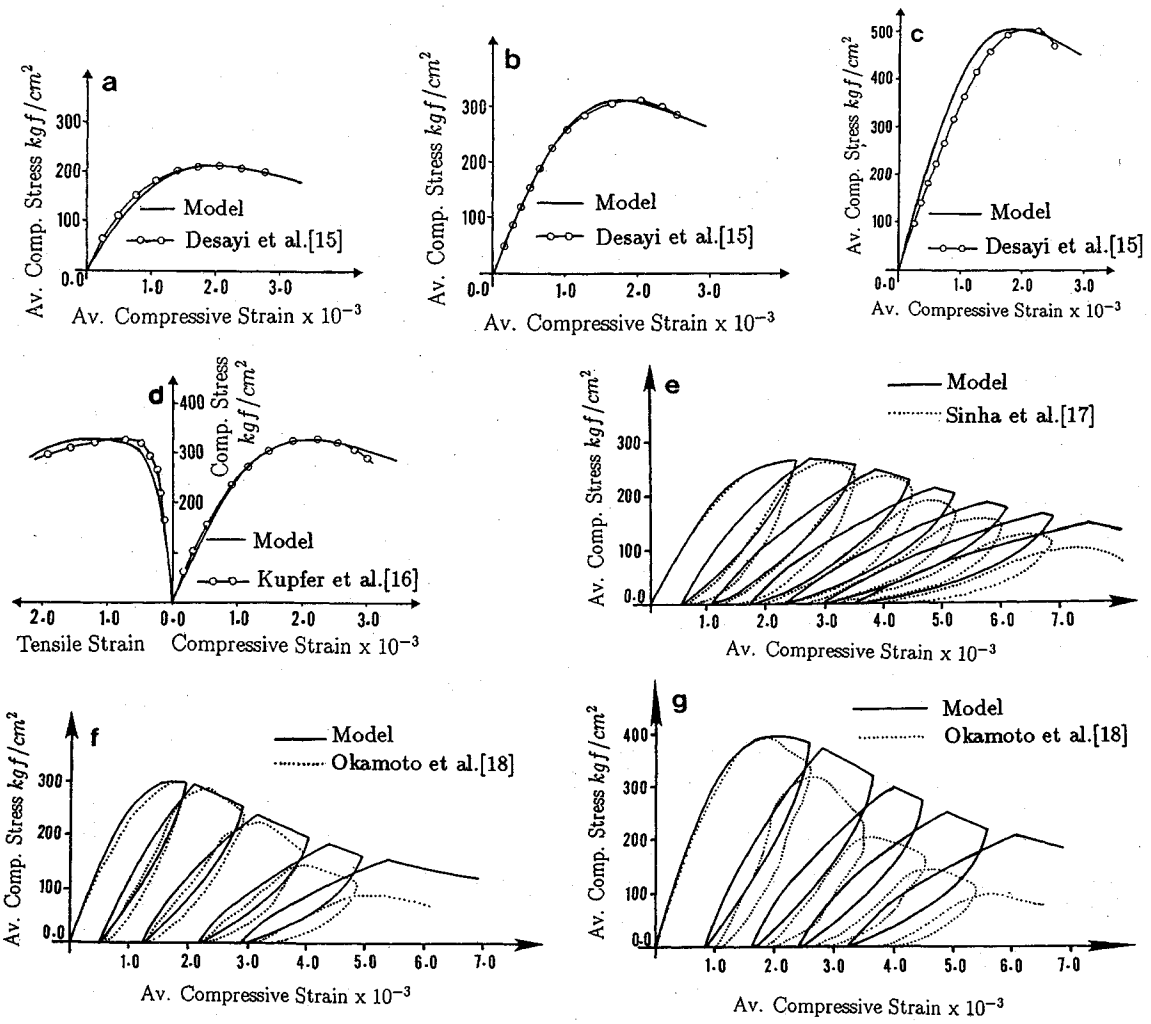

Fig.10 Comparison between Test Data and Model Results (Uniaxial Compression)

(3) UNIAXIAL COMPRESSION

In the same manner, in the beginning E_1, E_2 and λ are obtained using both Eq.(37) and the selected values in Section 4.(1). The value of $k_t=30\times10^4$ is kept constant while the value of the parameter k_c is changed to achieve the best fitting of the experimental data for concretes shown in **Fig.10**. From the experimental results, the peak compressive strength of these concretes a, b, c,...g are 212.0, 313.0, 506.0, 328.0, 260.0, 300.0 and 400.0, respectively. Also, the values of 10^{-4} E (E is the initial macroscopic stiffness) are 20.65, 32.86, 50.20, 29.50, 20.40, 32.00 and 37.50 kgf/cm², respectively. It was observed that the values of 10^{-3} k_c which are necessary to obtain reasonable fitting of the experimental data of concretes a, b, c,...g are 49.0, 58.0, 51.0, 42.0, 30.0, 58.0 and 45.0. The value of the parameter k_c can be obtained from the proposed relation in Section 4.(4). From **Fig.10**, a reasonable aggreement with test data is obtained, specially for the leteral loading as illustrated in **Fig.10**(d). On the other hand, in **Fig.10**(f and g), the model showed less softening behavior. This may be because of the assumption that the aggregate-aggregate contact behaves as a horizontal plateau which was proposed by Bazant et al.[4]. Therefore, the behavior should be modified to contain more softening.

(4) ESTIMATION OF THE PARAMETERS k_t AND k_c

Through the comparison with test data as explained in Section 4.(2) and 4.(3), the relation between k_t parameter and the tensile strength (f_t') for different values of Young's modulus is proposed. Moreover, the relation between k_c parameter and the compressive strength (f_c') is also obtained. These relations are shown in **Fig.11**. From **Fig.11**, it can be seen that as the value of tensile strength

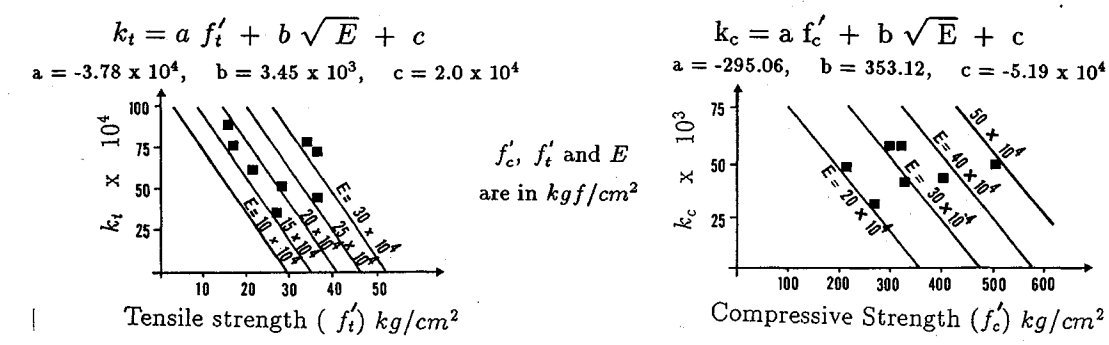

(a) k_t-f_t' Relationship at different values of Young's Modulus (E)

(b) k_c-f_c' Relationship at different values of Young's Modulus (E)

Fig.11 Estimation of k_t and k_c Parameters

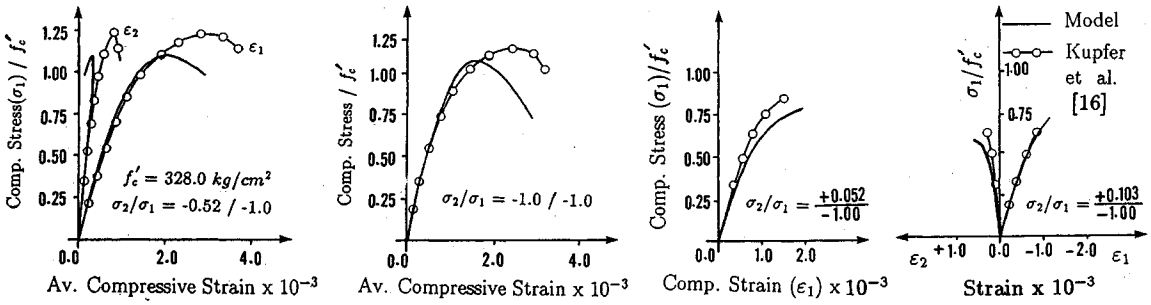

Fig.12 Comparison between Test Data and Model Results (Biaxial Loading)

increases, the value of k_t decreases. This may be due to the fact that as the macroscopic tensile strength increases the tensile strength of the contact at the microlevel increases. The tensile strength at the microlevel is controlled by k_t parameter as explained in Eqs.(18) and (20), in which the microscopic tensile strength decreases with the increase of k_t value. On the other hand, it is noticed that the variation of k_c parameter with the increase of the compressive strength is not too much. This may be because the compressive behavior at the microlevel is controlled by k_c parameter and the maximum compressive strength (σ_0 in Eq.(22)) at aggregate-aggregate contact. In addition, it seems the quality of the mortar in the experimental specimens is similar to each other.

(5) BIAXIAL LOADING

In **Fig.12**, the comparison between model results and the test data of ref.[10] are presented. The values of all parameters, as explained in Section **4.(1)**, are used. The values of $k_t = 65.40 \times 10^3$ and $k_c = 43.10 \times 10^3$ are also used. These values (k_t and k_c) are obtained from the proposed relations in Section **4.(4)**, which satisfy the uniaxial behavior. The macroscopic initial stiffness of these data is $E = 29.50 \times 10^4$ kgf/cm² and the compressive strength $f_c' = 328.0$ kgf/cm². As can be seen, although a reasonable agreement is obtained, less estimation of the maximum stresses in the case of biaxial compression is found. This may be because the values of the parameters k_t and k_c are over estimated.

5. CONCLUSIONS

In the present study, both the static and the cyclic behaviors of concrete are investigated based on the current modified micromechanical model. In the current model, concrete is idealized to have two types of particles ; aggregate and mortar. This idealization helps us to observe the behavior not only on the aggregate-aggregate contact as investigated before[4] but also on the aggregate-mortar contact. Moreover, the microstructure is considered to be nonhomogenous and the strain distribution is considered to be nonuniform. Based on the fitting of the available macroscopic experimental data using the present micromechanical model, a good agreement is obtained. This shows that the present model is capable of predicting the behavior of concrete. In particular, it can be concluded that :

(1) Through the proposed model, the relation between the initial macroscopic and microscopic stiffnesses is obtained. However, this relation is influenced by the nonhomogeniety of the microstructure and the nonuniformity of strain distribu-

tion.

(2) The macroscopic Poisson's ratio is found to be influenced by both the ratio between the normal and shear stiffnesses of the contact and the nonhomogeniety of the microstructure.

(3) In the current study, the proposed paths for cyclic loading were checked using the case of uniaxial loading and the case of cyclic tension with low compression. To have more general understanding of the cyclic behavior of concrete, a more comprehensive experimental work must be conducted not only on the macrolevel but also on the microlevel but with emphasis on the study on the more precise distribution of the contacts and also the strain distribution on the contacts.

REFERENCES

1) Bathurst, R.J. and Routhenburg, L. : Micromechanical Aspects of Isotropic Granular Assemblies with Linear Contact Interaction, Journal of Applied Mechanics, ASME, Vol.55, pp.17~23, March, 1988.
2) Chang, C.S. and Misa, A. : Theoretical and Experimental Study of Regular Packing of Granulars, Journal of Engineering Mechanics, ASCE, Vol.115, No.4, pp.704~720, April, 1989.
3) Christoffersen, J., Mehrabadi, M.M. and Nemat Nasser, S. : A Micromechanical Description of Granular Material Behavior, Journal of Applied Mechanics, ASME, Vol.48, pp.339~344, 1981.
4) Bazant, Z.P. and Oh, A.M. : Microplane Model for Progressive Fracture of Concrete and Rock, Journal of Engineering Mechanics, ASCE, Vol.111, No.4, pp.559~582, April, 1985.
5) Farahat, A.M., Wu, Z. and Tanabe, T. : Development of Microplane Model of concrete with Plural Types of Granular Particles, Proceeding of JSCE, 1991-08, No.433, Vol.15, pp.231~238.
6) Farahat, A.M., Wr, Z. and Tanabe, T. : Modified Microplane Model for Concrete Transaction of the Japan Concrete Institute, 1991, Vol.13, No.2, pp.109~116.
7) Mindlin, R.D. and Deresiewicz, H. : Elastic Spheres in Contact Under Varying Oblique Forces, Journal of Applied Mechanics, Trans. ASME, Vol.75, pp.327~344, September, 1953.
8) Hordijk, D.A. and Reinhardt, H.W. : Testing and Modeling of Plain Concrete Under Mode I Loading, Micromechanics of Failure of Quasi-Brittle Materials, eds. Shah, S.P., Swartz, S.E., and Wang, M., L., Elsvier Applied Science, pp.559~568, 1990.
9) Reinhardt, H.W. and Cornelissen, H.A.W. : Post Peak Cyclic Behavior of Concrete in Uniaxial Tension and Alternating Tensile and Compressive Loading, Journal of Cement and Concrete Research, Vol.14, No.2, pp.263~270, 1984.
10) Wolinski, S. : Influence of Aggregate Size on the Post-Peak Tensile Behavior of Concrete in Cyclic Tests, In Brittle Matrix Composites 2, eds. Brandt, A.M. and Marshall, I.H., Elsevier Applied Science, pp.496~505, 1989.
11) Yankelevsky, D.Z. and Reinhardt, H.W. : Uniaxial Behavior of Concrete in Cyclic Tension, Journal of Structural Engineering, ASCE, Vol.115, No.1, pp.166~182, January, 1989.
12) Yankelevsky, D.Z. and Reinhardt, H.W. : Model for Cyclic Compressive Behavior of Concrete, Journal of Structural Engineering, ASCE, Vol.113, No.1, pp.228~240, February, 1987.
13) Evans, R.H. and Marathe, M.S. : Microcracking and Stress-Strain Curves of Concrete in Tension, Materials and Structures (Paris), No.1, pp.61~64, Jan.-Feb., 1968.
14) Yankelevsky, D.Z. and Reinhardt, H.W. : Response of Plain Concrete to Cyclic Tension, Journal of American Concrete Institute, ACI Material, pp.365~373, September-October, 1987.
15) Desayi, P. and Krishnan, P. : Equation for Stress-Strain Curves of Concrete, Journal of American Concrete Institute, ACI, pp.345~350, March, 1964.
16) Kupfer, H. and Hilsdorf, H.K. : Behavior of Concrete Under Biaxial Stresses, Journal of American Concrete Institute, ACI, pp.345~350, March, 1964.
17) Sinha, B.P., Gerstle, K.H. and Tulin, L.G. : Stress-Strain Relations for Concrete Under Cyclic Loadings, Journal of American Concrete Institute, ACI, Vol.61, No.2, pp.195~211, 1964.
18) Okamoto, S., Shiomi, S. and Yamabe, K. : Earthquake Resistance of Prestressed Concrete Structures, Proceedings, Annual Convention, AIJ, pp.1251~1252, 1976.

(Received October 16. 1991)

繰り返し載荷を受けるコンクリートの微視力学的なモデル化

FARAHAT, Ahmed Mohamed・呉　智深・田辺忠顕

本論文は著者らによるコンクリートの単調載荷時での挙動に対して導入されたマイクロメカニカルモデルを修正し，繰り返し挙動を予測できるように拡張した．本モデルでは，Bazantの単一接触マイクロプレーンモデルとは違い，コンクリートを骨材-骨材もしくは骨材-モルタルというような2種類の接触を持つものとして理想化した．そしてその挙動は繰り返し荷重と単調載荷両方について調べられ区別された．さらにマイクロ的な非均質性や接触におけるひずみ分布の非均一性についても考慮した．そして実験データとの同定を行い，本モデルの妥当性を示した．